

Giant magnetoresistance in $\text{Cr}_{100-x}\text{Fe}_x$ bulk granular alloys

U. Brück, T. Schneider, M. Acet, and E. F. Wassermann

Tiefemperaturphysik, Gerhard-Mercator-Universität Duisburg, 47048 Duisburg, Germany

(Received 13 March 1995)

We report on the observation of giant magnetoresistance in magnetically inhomogeneous bulk granular $\text{Cr}_{100-x}\text{Fe}_x$ alloys. The largest magnetoresistance among the investigated alloys of $10.7 \leq x \leq 49.0$ at. % amounts to 26% for $x = 18.9$ at. % at 5 K and 4 T. This is substantially larger than in other bulk random 3d alloys and is of the same order of magnitude as that in granular films. Concentration, temperature, and field dependences of the magnetoresistance are also similar to those observed in granular media. The origin of giant magnetoresistance in bulk Cr-Fe is attributed to the field-induced alignment of Fe-rich ferromagnetic clusters in a Cr-rich matrix. Giant magnetoresistance in Fe-Cr collapses just above $x = 20$ at. %, at which long-range ferromagnetic order sets in.

The occurrence of giant magnetoresistance (GMR) in magnetic/nonmagnetic thin-film multilayers is generally attributed to spin-dependent scattering.^{1,2} The moments of initially antiferromagnetically coupled layers can be made to couple ferromagnetically by the application of an external magnetic field, leading to a reduction in the electrical resistance. Berkowitz *et al.*³ showed that GMR is not a property restricted to multilayers, but that it can also be found in granular Cu-Co films. More recent studies on granular films and ribbons have extended the list to the rapidly quenched alloys Ag-Co, Ag-Fe, Cu-Fe, Au-Fe, and Cr-Fe; all which are immiscible either in the solid state or even in the melt.⁴⁻⁷ On annealing they decompose rapidly and almost totally except for Cr-Fe, for which segregation kinetics are comparatively slow.⁸ Cr-Fe granular alloys are also unique in the sense that they can also be prepared in bulk form by conventional methods. This provides the possibility to extend the search for GMR effects to bulk granular material, which is undertaken in this work.

The phase diagram of $\text{Cr}_{100-x}\text{Fe}_x$ is shown in Fig. 1.⁹ A complete range of bcc (α) random solid solutions exists. A σ phase and a mixed $\alpha + \sigma$ phase are found, which are bounded by the dashed lines. The system also exhibits a miscibility gap for which the boundary is shown with the dashed-dotted line. Within the miscibility gap the system decomposes into Cr-rich α_1 and Fe-rich α_2 bcc phases. Alloys quenched to room temperature from the high-temperature random solid-solution region retain the bcc phase. However, complete randomness is not preserved, as evidenced by Mössbauer,¹⁰⁻¹⁴ diffuse neutron scattering,^{15,16} and isochronal annealing¹⁷ experiments. The results of these measurements show the presence of Fe-rich and Cr-rich clustering on a length scale of ~ 2 nm for $x \approx 25$ at. %, which is due to segregation during quenching. This property gives the granular character to bulk Cr-Fe alloys. The magnetic phase diagram for quenched alloys is shown by the solid lines in Fig. 1.^{18,19} On the Fe-rich ferromagnetic (FM) end the Curie temperature T_C decreases with increasing Cr concentration up to $x \approx 20$ at. %. A cluster-glass-like frustrated state with freezing temperature T_f is observed for $10 < x < 30$ at. %.

The boundaries of this state are uncertain near the onset of ferromagnetism. Antiferromagnetic (AF) order sets in below $x \approx 18$ at. % and the Néel temperature increases with decreasing x . The critical region is expanded in the inset.

$\text{Cr}_{100-x}\text{Fe}_x$ alloys were prepared by arc melting under argon atmosphere and cut to samples $6 \times 2 \times 0.2$ mm³. After annealing at 1200 K the samples were quenched into water at room temperature. Concentrations were determined by microprobe analysis to be 10.7, 17.0, 18.6, 18.9, 29.2, and 49.0 at. %. Magnetoresistance measurements in magnetic fields B up to 4 T were made by a standard four-point technique. Both longitudinal MR,

$$\Delta\rho_{\parallel}/\rho_0 = [\rho_{\parallel}(H, T) - \rho(0, T)] / \rho(0, T),$$

and transverse MR,

$$\Delta\rho_{\perp}/\rho_0 = [\rho_{\perp}(H, T) - \rho(0, T)] / \rho(0, T),$$

where $\rho_0 \equiv \rho(0, T)$, were measured in increasing and decreasing external field.

Figure 2 shows $\Delta\rho/\rho_0$ vs B curves for $x = 18.9$ at. % at various temperatures. This sample shows the largest MR among all others presently investigated amounting to 26% at 4 T and 5 K; a value which is the largest encountered in bulk granular alloys and, in fact, somewhat larger than the 20% GMR effect of Fe-Cr granular films at a similar temperature and magnetic field.⁷ At all temperatures $\Delta\rho/\rho_0$ is always negative and no saturation occurs in fields up to 4 T. Hysteresis is also not found and the anisotropy $(\Delta\rho_{\parallel} - \Delta\rho_{\perp})/\rho_0$ is less than 0.5%.

$\Delta\rho/\rho_0$ vs B at 5 K for all samples is plotted in Fig. 3. The MR of samples with $10.7 \leq x \leq 18.9$ at. % has similar field dependence in that the slope always decreases with increasing field. At 4 T the MR increases with increasing concentration from 11% to 26% and at $x = 29$ at. %, for which the field dependence is highly weakened, the MR decreases rapidly. For $x = 49.0$ at. % $\Delta\rho_{\parallel}/\rho_0$ and $\Delta\rho_{\perp}/\rho_0$ are both plotted. This sample shows a relatively large anisotropy amounting to 4% and a weak field dependence of less than 0.5% for $0.2 < B < 4$ T. The large anisotropy, which is correlated to the alignment of

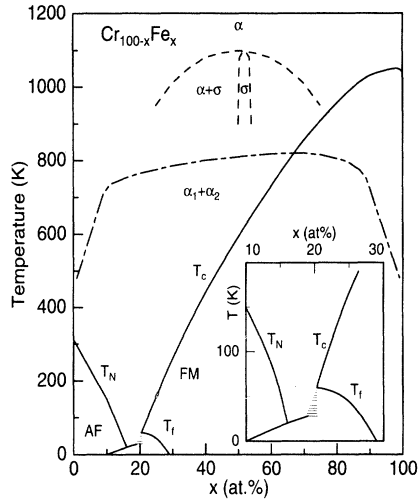


FIG. 1. The structural and magnetic phase diagram of $\text{Cr}_{100-x}\text{Fe}_x$. The mixed $\alpha + \sigma$ phase and the σ phase are bounded by the dashed lines. The borders of the miscibility gap, within which the system segregates to α_1 and α_2 , are shown by the dot-dashed line. The magnetic transformation temperatures are shown by full lines. The critical region is shown in the inset.

the domains in low magnetic fields, as well as the weak dependence in higher fields, is typical of "normal" ferromagnets such as Fe or Ni.

Figure 4 shows $|\Delta\rho/\rho_0|$ vs T . The MR of alloys with $10.7 \leq x \leq 18.9$ at. % increases with decreasing temperature. The increase becomes steeper as the temperature is lowered and the temperature dependence is weakened with decreasing concentration. The MR of $x = 29.2$ at. % is almost temperature independent and that of $x = 49$ at. % (not shown) practically vanishes. Up to $x = 18.9$ at. % the curves are comparable in form and magnitude to, e.g., those of as-prepared Cu-Co granular films.³

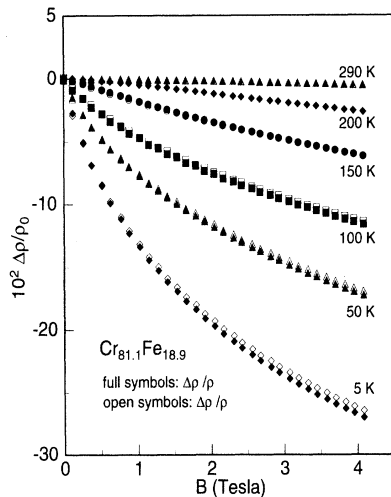


FIG. 2. $\Delta\rho/\rho_0$ vs B at various temperatures for $x = 18.9$ at. %. The MR at 5 K is of the same magnitude as the GMR effect in granular media. The anisotropy is negligible.

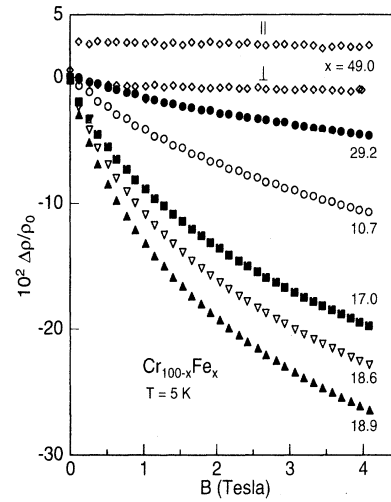


FIG. 3. $\Delta\rho/\rho_0$ vs B at 5 K for $\text{Cr}_{100-x}\text{Fe}_x$. Since the anisotropy at small only longitudinal MR is shown except for $x = 49.0$ at. %, for which both longitudinal (\parallel) and transverse (\perp) MR are shown.

Figure 5 shows the absolute value of the MR as a function of Fe concentration at 4 T and several fixed temperatures. The data of Hedgcock, Strom-Olsen, and Wilford,²⁰ for $x = 3$ and 5 at. % (open triangles) and Banerjee and Raychandhuri²¹ for $x = 25$ at. % (asterisk) are also shown. The MR shows a steep increase with increasing Fe concentration up to $x \approx 20$ at. % after which it drops rapidly. The rapid drop is sketched by the broken line only for $T = 5$ K for clarity. The behavior of the concentration dependence of the MR is temperature sensitive for $x < 20$ at. %, while for $x > 20$ at. % it is insensitive to temperature. A comparison of Fig. 5 with the magnetic phase diagram indicates that the MR reaches its max-

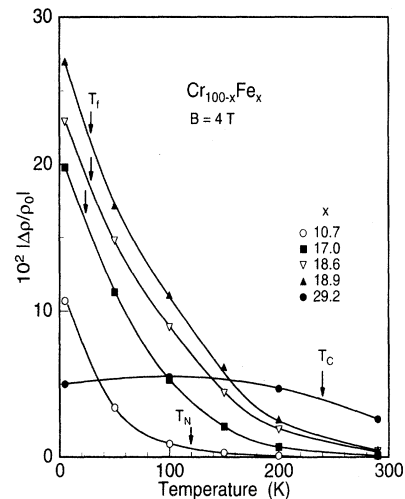


FIG. 4. $\Delta\rho/\rho_0$ vs T for $\text{Cr}_{100-x}\text{Fe}_x$. The temperature dependence is highly weakened as the Fe concentration approaches the onset of long-range FM order. The arrows point to the magnetic transformation temperatures. The lines are guides.

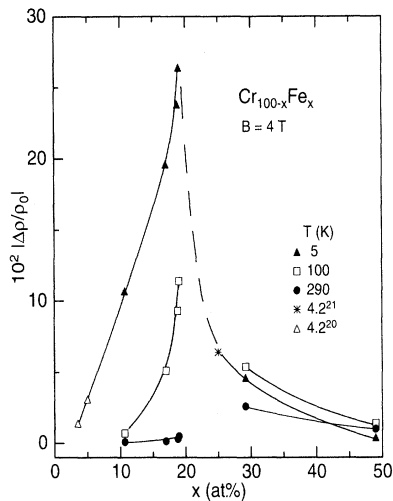


FIG. 5. Longitudinal magnetoresistance as a function of Fe content for $\text{Cr}_{100-x}\text{Fe}_x$ at 4 T. Data at 4.2 K of Refs. 20 and 21 are also included. The lines are guides. The sharp decrease for $T = 5$ K is shown by the dashed line.

imum in the cluster-glass region and therefore it may be appealing to relate the observed effects to spin-glass properties. However, there are significant differences between the behavior of the MR of Cr-Fe cluster glasses and other spin-glass alloys. The negative MR of canonical spin glasses (Au-Fe, Au-Mn, etc.) is governed by $|\Delta\rho/\rho| \propto H^n$ ($n \approx 2$), which gives an increasing slope for $|\Delta\rho/\rho|$ with increasing field.²² Moreover, $\Delta\rho/\rho$ in spin glasses is only $\sim 1\%$ at 1 T and there are hysteresis effects. In ternary spin-glass alloys such as $\text{Fe}_x\text{Ni}_{80-x}\text{Cr}_{20}$ ($16 < x < 21$ at.%) the MR amounts to only 5×10^{-3} at 4 T and 4.2 K.²¹

As opposed to the dissimilarities to spin glasses several features of the observed phenomena are similar to the GMR effect in granular films. The slope of $|\Delta\rho/\rho|$ de-

creases with increasing field and no saturation of the MR occurs at 4 T. The anisotropy is negligible and the position of the MR maximum at $x \approx 20$ at. % is similar to that found in a variety of granular films.^{5,7} The 26% GMR effect at 4 K at $x = 18.9\%$ agrees especially well with the results on Fe-Cr granular films.⁷ In view of these similarities the GMR effect in Fe-Cr bulk alloys and granular films is expected to be of the same origin.

The cluster-glass concentration region of Fe-Cr is composed of Fe-rich FM granules in a Cr-rich environment. The Fe-rich granules are among themselves noninteracting entities, and therefore the overall sample is initially in a superparamagnetic state. An external field places the system in a final state where the moments align, thereby leading to a decrease in the resistance. This persists up to a concentration near the onset of long range FM order, above which there is little difference in the degree of alignment between the initial and final states. Thus an external field has hardly any influence on changing the resistance. As a consequence the MR drops rapidly and remains concentration and temperature insensitive, as seen in Fig. 5.

The strong increase of $|\Delta\rho/\rho_0|$ with decreasing temperature below ~ 20 at. % is due to the increased tendency of alignment of the moments of the granules in an external field. This behavior should be closely related to the temperature dependence of the magnetization. However, no assessment of this relation is made here since magnetization measurements on exactly the same samples are required to understand this highly concentration-sensitive phenomenon in Cr-Fe. Nevertheless, the present results demonstrate that the form and size of GMR effects of Cr-Fe quenched-state bulk alloys and granular films are very similar.

We are grateful to W. Pepperhoff for valuable suggestions. This work was supported by the Deutsche Forschungsgemeinschaft (SFB 166).

¹M. N. Baibich, J. M. Broto, A. Fert, F. Nguyen Van Dau, F. Petroff, P. Eitenne, G. Creuzet, A. Friederich, and J. Chazelas, *Phys. Rev. Lett.* **61**, 2472 (1988).
²S. S. P. Parkin, *Phys. Rev. Lett.* **71**, 1641 (1993).
³A. E. Berkowitz, J. R. Mitchell, M. J. Carey, A. P. Young, S. Zhang, F. E. Spada, F. T. Parker, A. Hutten, and G. Thomas, *Phys. Rev. Lett.* **68**, 3745 (1992).
⁴J. Q. Xiao, J. S. Jiang, and C. L. Chien, *Phys. Rev. Lett.* **68**, 3749 (1992).
⁵C. L. Chien, J. Q. Xiao, and J. S. Jiang, *J. Appl. Phys.* **73**, 5309 (1992).
⁶L. H. Chen, S. Jin, J. H. Tiefel, S. H. Chang, M. Eibschutz, and R. Ramesh, *Phys. Rev. B* **49**, 9194 (1994).
⁷K. Takanashi, T. Sugawara, K. Hono, and H. Fujimori, *J. Appl. Phys.* **76**, 6790 (1994).
⁸T. Schneider, M. Acet, and E. F. Wasserman, *J. Appl. Phys.* **70**, 6559 (1991).
⁹O. Kubaschewski, *Iron-Binary Phase Diagrams* (Springer-Verlag, Berlin, 1982).
¹⁰H. H. Ettwig and W. Pepperhoff, *Arch. Eisenhüttenwes.* **41**, 471 (1970).
¹¹J. Hesse and A. Rübartsch, *Physica B+C* **80B**, 33 (1975).

¹²M. Shiga and Nakamura, *J. Phys. Soc. Jpn.* **49**, 528 (1980).
¹³W. M. Xu, W. Steiner, M. Reissner, A. Pösinger, M. Acet, and W. Pepperhoff, *J. Magn. Magn. Mater.* **104-107**, 2023 (1992).
¹⁴W. M. Xu, A. Pösinger, R. Wagoner, M. Reissner, W. Steiner, G. Wiesinger, and M. Acet, *Hyperfine Interact.* **94**, 1843 (1994).
¹⁵A. T. Aldred, *Phys. Rev. B* **14**, 219 (1976).
¹⁶A. T. Aldred, B. D. Rainford, J. S. Kouvel, and T. J. Hicks, *Phys. Rev. B* **14**, 228 (1976).
¹⁷F. Richter, W. Bendick, and W. Pepperhoff, *Z. Metallkde* **65**, 42 (1974).
¹⁸S. K. Burke and B. D. Rainford, *J. Phys. F* **13**, 441 (1983).
¹⁹S. K. Burke, R. Cywinski, J. R. Davis, and B. D. Rainford, *J. Phys. F* **13**, 451 (1983).
²⁰F. T. Hedgcock, J. O. Strom-Olsen, and D. F. Wilford, *J. Phys. F* **7**, 855 (1977).
²¹S. Banerjee and A. K. Raychaudhuri, *J. Phys. Condens. Matter* **5**, L295 (1993).
²²A. K. Nigam and A. K. Majumdar, *Phys. Rev. B* **27**, 495 (1983).